



Laser Anemometry Based on Collective Scattering: the Effects of Propagating and Nonpropagating Fluctuations

Lars Lading^a, Mark Saffman^a & Robert V. Edwards^b

^aRisø National Laboratory, Association Euratom Optics and Fluid Dynamics Department, DK-4000 Roskilde, Denmark

^bChemical Engineering Department, Case Western Reserve University, Cleveland, OH 44106, USA

(Received 14 February 1996; accepted 3 July 1996)

ABSTRACT

Laser anemometry, as it is commonly applied, requires particles. However, in certain types of high-speed flows and plasma flows no particles are present. Collective light-scattering may then be applied to measure fluid or plasma velocity. A new hybrid scheme has been proposed; the scheme allows for better axial resolution than that which has previously been demonstrated. The effects of propagating and nonpropagating fluctuations on the expected cross-correlation functions are investigated. The correlation function will, in general, be asymmetric and will consist of three identifiable peaks: two caused by (counter) propagating fluctuations and one caused by nonpropagating fluctuations. Thermal diffusivity causes the maximum of the 'nonpropagating peak' to be displaced relative to the case of no diffusivity. © 1997 Elsevier Science Ltd.

1 INTRODUCTION

Quasi-elastic scattering is the basis for most types of laser anemometry. A possible shift in frequency is only caused by the movement (velocity) of the scatterer and not by a change in the quantum mechanical state of the particle. This type of scattering is also used for measuring diffusion and molecular dynamics. Laser anemometry (LA), as it is commonly applied, requires that small particles be suspended in the fluid. Measuring fluid velocity on the basis of molecular scattering is, in general, not considered feasible because the thermal velocities of the molecules are often much larger than the fluid velocity. Incoherent molecular scattering will normally give a spectral broadening proportional to the thermal velocity of

the molecules. In most flows, this type of broadening is much larger than the fluid velocity, thus making it unsuited for anemometry.

Despite the large thermal velocity of molecules collective light-scattering may provide a signal with a spectral width much smaller than the thermal broadening. Collective scattering is scattering from a large number of scatterers that in some way support a large-scale (large compared with the mean free path) scattering structure. A sound-wave may be an example of such a wave structure. It is necessary that the spatial scale of the structure is larger than the mean free path. The spatial probe scale has to match the scale of the collective structure. The code of the anemometer (the intensity distribution in the measuring volume as seen from the detector(s)) defines which spatial refractive index structures contribute to the signals.

Collective light-scattering is not constrained by the thermal motion of the molecules, but can be considered as based on scattering or diffraction from refractive index fluctuations. A number of conflicting requirements have to be fulfilled in order to make a useful system. We have recently proposed a so-called hybrid system that combines a reference beam Doppler configuration with a time-of-flight anemometer.^{1,2}

Refractive index fluctuations can be divided into two categories: propagating and nonpropagating fluctuations. Sound waves are examples of propagating fluctuations. They propagate in the fluid and thus have a velocity relative to a fixed reference given by the fluid velocity plus (or minus) the sound velocity. Nonpropagating waves are intrinsically preferable for fluid velocity measurements due to the fact that their movement is exclusively given by the convection of the fluid.

Velocity information may be inferred from a crosscorrelation function. We have investigated the crosscorrelation function of the envelopes of the detector signals; both propagating and nonpropagating fluctuations are incorporated. The correlation function will in general be asymmetric and will consist of three identifiable peaks: two caused by (counter) propagating fluctuations and one caused by nonpropagating fluctuations. Thermal diffusivity causes the maximum of the 'nonpropagating peak' to be displaced relative to the case of no diffusivity.

2 SYSTEM MODEL

The system that is being investigated is a combination of a reference beam laser Doppler anemometer (LDA) and a laser time-of-flight anemometer (LTA) as illustrated in Fig. 1. This hybrid makes it possible to achieve the good axial spatial resolution of the LTV and at the same time apply

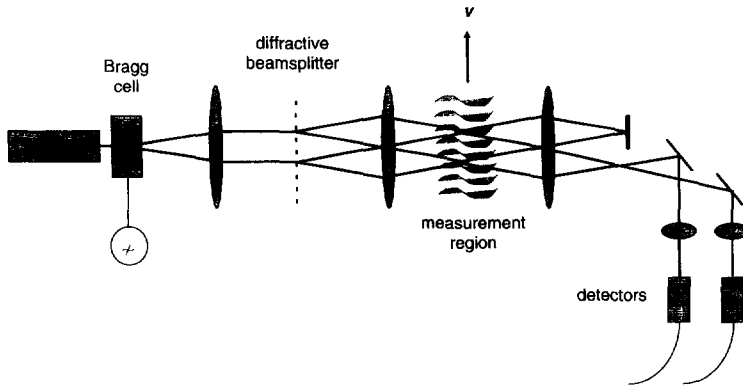


Fig. 1. Hybrid configuration for nonparticle laser anemometry. The reference beams are introduced with a small angular offset in order to ensure the mixing and spatial highpass filtering.

reference beam detection.^{1,2} For a laser anemometer we can define a *code* that is a function that determines the way in which the velocity information is encoded into the system: for an LDA the code is a wave packet; for an LTA it consists of two displaced peaks. The code of the hybrid system is shown in Fig. 2. It consists of two displaced wave packets each with only a few oscillations.

A spatial turbulence spectrum is shown in Fig. 3. Also shown are the 'filters' of the LDA and the hybrid system, respectively. The filters select the spectral regions from which refractive index perturbations can contribute to the signal. It is seen that the LDA selects a much narrower

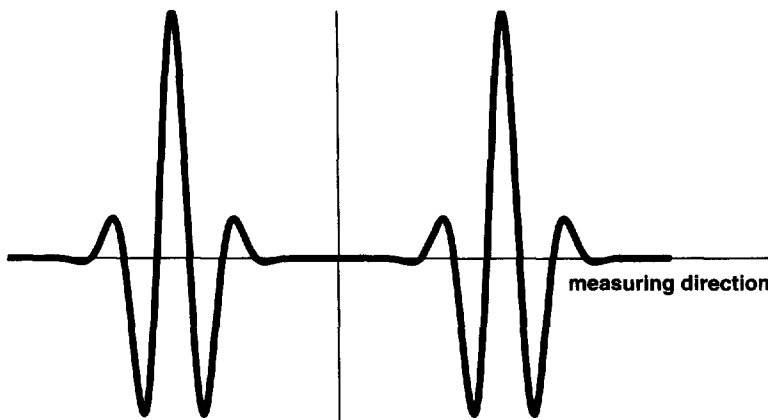


Fig. 2. The intensity distribution (deviation from the mean) as seen by the detectors of a hybrid laser anemometer, which defines the *code* of the system.

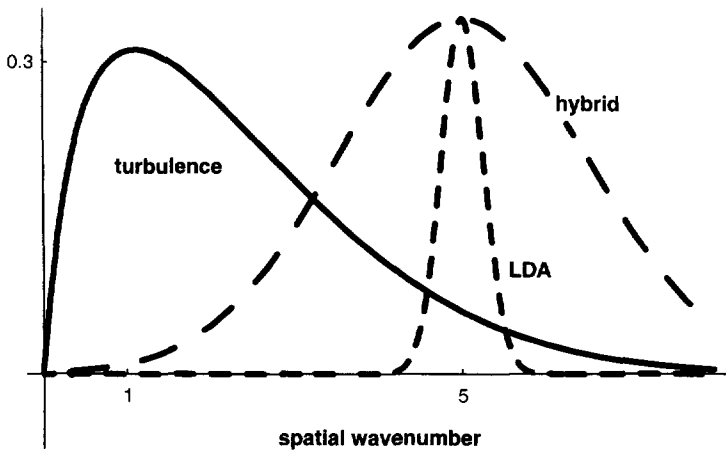


Fig. 3. A turbulence spectrum (solid line) with the filter functions of an LDA (the narrow filter) and a hybrid LA, respectively. Notice that the hybrid utilises a much larger part of the turbulence spectrum.

region than the hybrid system. For a given spatial resolution this implies that the hybrid will give a much stronger signal. However, if the purpose of a given experiment is to investigate the propagation of different spatial wave numbers, a narrow spatial frequency range is mandatory. For 'frozen' turbulence a large spectral region must be preferable.

In discussing the spectral regions of the turbulence spectrum we must remember that the purpose may be to obtain information about the turbulence, possibly about its temporal evolution. With the present scheme we can only 'track' turbulence in a spectral region below that which gives rise to the signal: the high frequency turbulence serves the same purpose as particles do in normal laser anemometry.

2.1 Signal processing

The signals encountered here have similarities with signals of a laser anemometer with many particles in the measuring volume. It is a continuous signal that exhibits fluctuations caused by the randomness of the scattering object. However, the processing is somewhat different. It consists of a fast analog front end followed by a digital correlator. The general scheme is shown in Fig. 4. The analog processing incorporates bandpass filters to reduce the noise and to ensure that only the dynamic parts of the signals are passed on to the envelope detectors. These detectors eliminate the effect of phase differences between the wave packets of the two focal volumes. The front end scheme is illustrated in Fig. 5. The delay is chosen to be larger than the coherence time of the

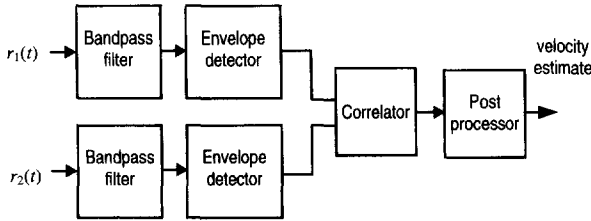


Fig. 4. Signal processing scheme for the hybrid configuration. The envelope detectors are used in order to make the system insensitive to small optical phase errors. The postprocessor is in general assumed to do a curve fitting from which relevant parameters are taken.

noise, but smaller than the period of the signal oscillation. Such a scheme makes the expected output insensitive to noise. (The uncertainty caused by noise cannot be removed.) The expected correlation function may be rather complex. Thus the actual parameter extraction will be performed on the basis of a curve fitting procedure.

2.2 Correlation functions

The correlation function of the detector signal of one channel is given by³

$${}^{(1)}R(\tau) \propto \int_{x-y \text{ plane}} S(\mathbf{k}, \tau) F(\mathbf{k})^2 d\mathbf{k} \tag{1}$$

where $S(\mathbf{k}, \tau)$ is the 2-D spatial Fourier transform of the 2-D space-time correlation for the phase perturbations ($\mathbf{k} = (k_x, k_y)$). $|F(\mathbf{k})|^2$ is an instrument function given by the modulated part of the field distribution in the measuring volume: the code shown in Fig. 2.

In the signal processing we estimate the square of the envelope. This is done in a way that is mathematically equivalent to estimating the absolute square of the *complex* signal, but note that the real and the imaginary parts are not independent. The correlation function for the squared signal, the second-order correlation ${}^{(2)}R(\tau)$, can be evaluated directly from the

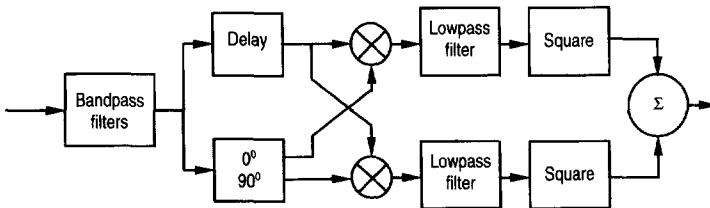


Fig. 5. Block diagram of the prefiltering and envelope detection (only one channel is shown).

first-order correlation of the envelopes assuming Gaussian statistics for the (nonsquared) signals. We find that⁴

$${}^{(2)}R(\tau) = ({}^{(1)}R(0))^2 + 2({}^{(1)}R(\tau))^2 \quad (2)$$

The cross-correlation is essentially given by a displaced version of eqn (2), if we assume a constant convection velocity and that the decay time of the thermal fluctuations is much longer than the time-of-flight. If this is not the case, we apply the double peaked function for $F(\mathbf{k})$ and use only the displaced parts.

If the convective flow is turbulent, the autocorrelation function is modified to incorporate the effect of velocity fluctuations. The crosscorrelation function may then be evaluated by the following expression

$${}^{(2)}R_c(\tau) = \int_{\text{all } \mathbf{v}} {}^{(2)}R_c(\tau, \mathbf{v}) dP(\mathbf{v}) \quad (3)$$

where $P(\mathbf{v})$ is the probability distribution for \mathbf{v} .

In order to evaluate the correlation function given by eqn (1) we need an expression for $S(\mathbf{k}, \tau)$.

3 PROPAGATING AND NONPROPAGATING FLUCTUATIONS

Turbulence will inevitably cause refractive index fluctuations. The fluctuations may be convected by the fluid motion or they may propagate as sound waves. The nonpropagating (relative to the fluid) waves are preferable for inferring the fluid velocity, but unfortunately, they do in general have a shorter coherence time than the propagating fluctuations.

Let $n(\mathbf{r}, t)$ = the index of refraction as a function of space and time. We can then write

$$dn = \beta_1 dT + \beta_2 dP \quad (4)$$

where T and P are the local temperature and pressure, respectively, and β_1 and β_2 are constants. The equation for the energy balance in a moving, compressible fluid is⁵

$$\rho \hat{C}_p \left(\frac{\partial(T - T_0)}{\partial t} + \mathbf{v} \cdot \nabla(T - T_0) \right) = \alpha \rho \hat{C}_p \nabla^2(T - T_0) - \left(\frac{\partial p}{\partial t} + \mathbf{v} \cdot \nabla p \right) \quad (5)$$

Here, we have assumed that no temperature fluctuations are generated by viscous dissipation in the region of interest, but that the temperature fluctuations are convected into the region of interest by the flow (T_0 is the mean temperature and p is the fluctuating part of the pressure). The pressure terms are sound-waves propagating through the region of interest. If the pressure terms are rewritten in terms of the local density,

ρ , the time axis is shifted by τ , and the spatial Fourier transform is taken of the entire equation, we obtain

$$\frac{\partial \hat{\Theta}(\mathbf{k}, t + \tau)}{\partial \tau} - i\mathbf{k} \cdot \mathbf{v} \hat{\Theta}(\mathbf{k}, t + \tau) = -k^2 \alpha \hat{\Theta}(\mathbf{k}, t + \tau) - \frac{p_0 \gamma \delta \omega}{2\rho_0 \hat{C}_p} e^{-i\mathbf{k} \cdot (\mathbf{v} + \mathbf{v}_s)(t + \tau)} \quad (6)$$

where $\hat{\Theta}$ is the spatial Fourier transform of the temperature variations, $\delta\omega$ is the Fourier transform of p , α is the thermal diffusivity, γ is the ratio of heat capacities, and \hat{C}_p is the heat capacity per mass of the fluid. The propagation of the sound waves at velocity \mathbf{v}_s is now explicit. The desired autocorrelation of the space-time fluctuations in the temperature is obtained by multiplying this equation by the Fourier transform of the temperature field and then taking the expected value of the result, namely:

$$\begin{aligned} \frac{\partial \hat{\Theta}(\mathbf{k}, t) \hat{\Theta}(\mathbf{k}, t + \tau)}{\partial \tau} - i\mathbf{k} \cdot \mathbf{v} \hat{\Theta}(\mathbf{k}, t) \hat{\Theta}(\mathbf{k}, t + \tau) \\ = -k^2 \alpha \hat{\Theta}(\mathbf{k}, t) \hat{\Theta}(\mathbf{k}, t + \tau) - \frac{p_0 \gamma \delta \omega}{2\rho_0 \hat{C}_p} e^{-i\mathbf{k} \cdot (\mathbf{v} + \mathbf{v}_s)(t + \tau)} \hat{\Theta}(\mathbf{k}, t) \end{aligned} \quad (7)$$

In taking the expected value, we need to make two more reasonable assumptions: (1) the flow velocity is constant for the time it takes a structure to move through the region of interest. This assumption is usually a very reasonable one for laser anemometer analysis and is claimed here; (2) the sound-wave fluctuations are not correlated in time with the thermal fluctuations. Indeed, it is reasonable to assume that the two fluctuations arise from different sources outside the region of interest. Using the above assumptions, for the temperature fluctuation correlation C_{TT} we get

$$\frac{\partial C_{TT}(\mathbf{k}, \tau)}{\partial \tau} - i\mathbf{k} \cdot \mathbf{v} C_{TT}(\mathbf{k}, \tau) = -k^2 \alpha C_{TT}(\mathbf{k}, \tau) \quad (8)$$

The solution is

$$C_{TT}(\mathbf{k}, \tau) = C_{TT}(\mathbf{k}, 0) \exp[i\mathbf{k} \cdot \mathbf{v} \tau] \exp[-k^2 \alpha \tau] \quad (9)$$

The pressure fluctuation correlation, $\Pi(\mathbf{k}, \tau)$, can be calculated in a similar manner. The authors are uncertain as to the decay scale of the sound-waves, but believe it should behave similarly to the decay of the thermal waves. Overall, this yields an index of refraction correlation function of the form

$$S(\mathbf{k}, \tau) = \varepsilon_1^2 \exp[i\mathbf{k} \cdot \bar{\mathbf{v}} \tau] \exp[-k^2 \alpha \tau] + \varepsilon_2^2 \exp[+i\mathbf{k} \cdot (\bar{\mathbf{v}} \pm \mathbf{v}_s) \tau] d(\tau) \quad (10)$$

where $d(\tau)$ is the decay term associated with the sound-waves.

This expression goes into eqn (1) to calculate the expected output of the photon experiment. Roughly, the frequency spectrum of the index of refraction fluctuations detected in the scattering experiment has three peaks, one centred at $\mathbf{k} \cdot \bar{\mathbf{v}}$ (Rayleigh peak) due to the thermal fluctuations convected through the region of interest having a minimum width $k^2 \alpha$, and two sound-wave peaks (Brillouin peaks) displaced from the thermal peak by $\pm \mathbf{k} \cdot \mathbf{v}_s$. The instrument function in eqn (1) created by the optics of a particular light scattering experiment broadens the peaks, but essentially leaves the centre frequencies of the peaks intact. A successful experiment will require that the optical parameters, such as the scattering vector and the spatial bandwidth of the instrument function, be picked so that the intrinsic broadening of the peaks does not obscure the frequency shift.

4 THE CROSSCORRELATION FUNCTION

We can now evaluate the crosscorrelation based on eqns (3) and (10). We have done that partly by symbolic evaluations (using *Mathematica*), partly by numerical calculations. Figures 6–11 show the calculated crosscorrelation function for different assumptions, as described in the captions. Based on the measurements presented by Bonnet *et al.*,⁶ we assume

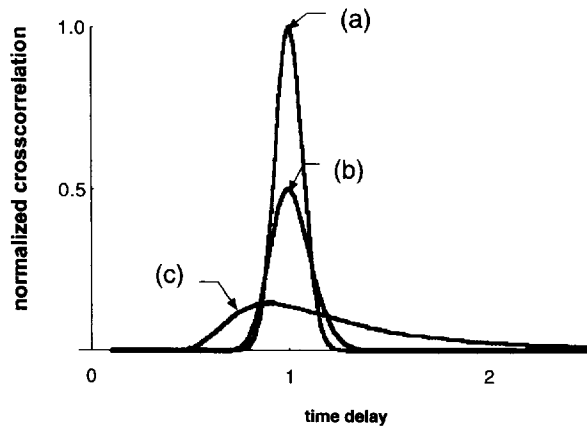


Fig. 6. Crosscorrelation functions assuming that all fluctuations are nonpropagating and only convected by the fluid motion. Case (a) is for a constant convection velocity; (b) is for a Gaussian probability density with a s.d. of 0.1 for the velocity; and (c) is for a s.d. of 0.5. Note the decrease in the correlation maximum and the displacement of the peak with increasing velocity fluctuations. It is assumed that the thermal diffusivity is negligible. The functions are normalised with the maximum crosscorrelation value and plotted as functions of the time-lag normalised with the time-of-flight corresponding to the mean velocity.

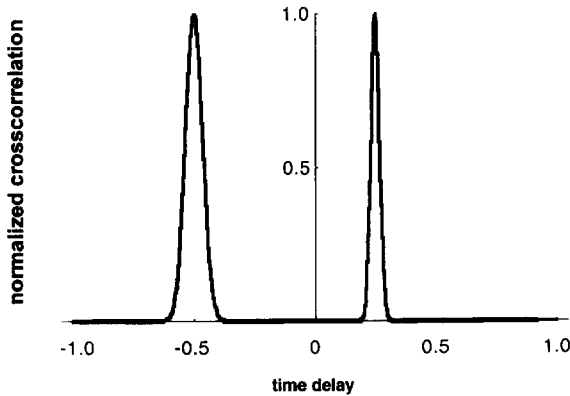


Fig. 7. Crosscorrelation function assuming that only propagating fluctuations (sound waves) contribute to the signals. The propagation speed is assumed to be three times the convection velocity, which is assumed to be constant. Note that the counterpropagating sound wave causes a peak at a displacement of opposite sign relative to the convection displacement, which is given by the value '1'. The Mach no. is 0.33.

that the power of the signals caused by the propagating modes is in general smaller than the power of the signals caused by the convected fluctuations.

We note that the peak of the slowest velocity component appears to be smeared faster than the peaks of the faster components. The complete crosscorrelation may be quite complicated. If the convection velocity and the sound velocity are very different, it is not possible to identify which parts of the function are caused by the different types of fluctuations of

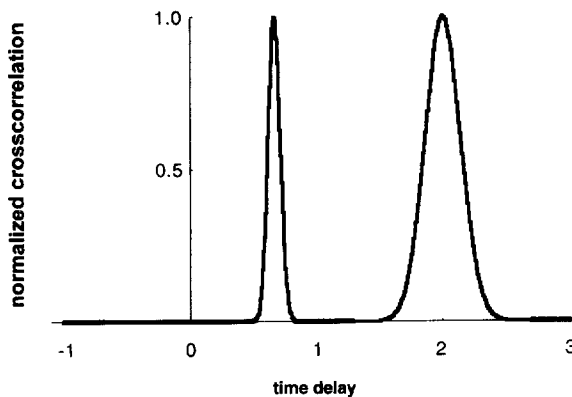


Fig. 8. Crosscorrelation function assuming that only propagating fluctuations (sound waves) contribute to the signals (as in Fig. 7), but the propagation speed is now assumed to be half the convection velocity, which is assumed to be constant. Note that the counterpropagating sound wave causes a peak at a displacement of opposite sign relative to the convection displacement, which is given by the value '1'. The Mach no. is 2.

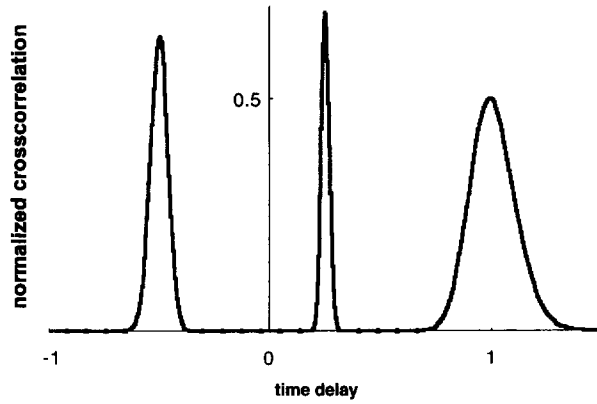


Fig. 9. Correlation function assuming both propagating and nonpropagating fluctuations of the same initial power. The s.d. of the convection velocity is 0.1. The Mach no. is 0.33.

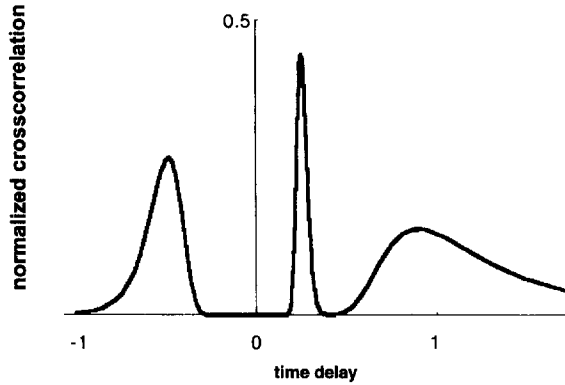


Fig. 10. Correlation function assuming both propagating and nonpropagating fluctuations of the same initial power. The s.d. of the convection velocity is 0.5. The Mach no. is 0.33.

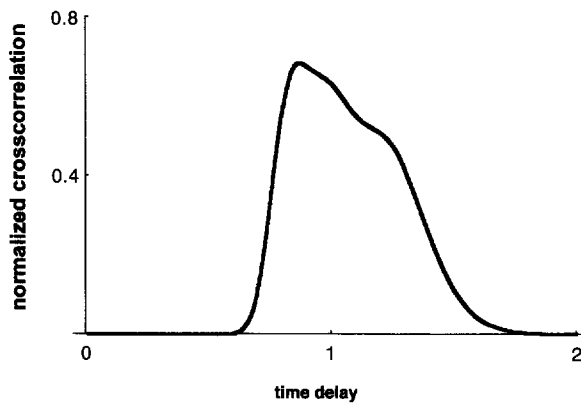


Fig. 11. As Fig. 10 but with a Mach no. of 4.

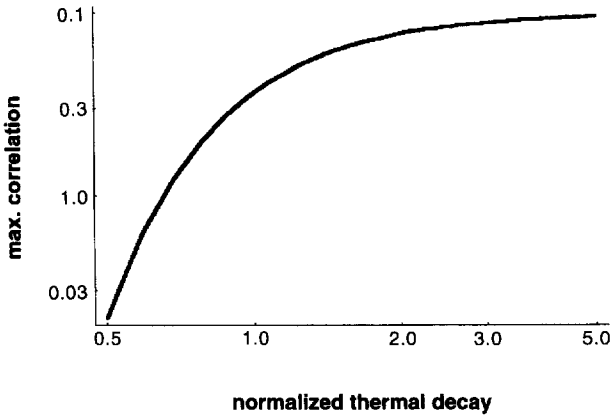


Fig. 12. The maximum crosscorrelation for the ‘convected’ part vs the thermal decay normalised with the time-of-flight assuming that the width of each wave packet of the code is 0.1 times the spacing between the two packets.

the refractive index of the fluid. Thus, an estimation of the velocity parameters must generally be performed by fitting the observed correlation function to a model function.

The effect of the thermal decay of the refractive index pattern is illustrated in Fig. 12. The case of an infinitely large decay corresponds to Taylor’s frozen pattern hypothesis. The correlation function is also affected by thermal decay. This is illustrated in Fig. 13. The displacement

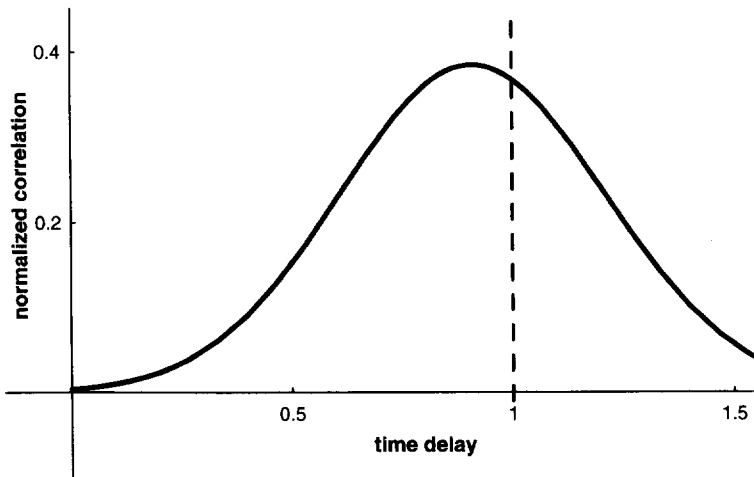


Fig. 13. The crosscorrelation assuming a constant convection velocity but a decay time of the turbulence structure equal to the time-of-flight between the two illuminated regions. Note that the peak of the correlation is displaced to a time lag shorter than the true time-of-flight.

of the correlation peak to a shorter time lag can be explained by noting that structures convected the shortest distance will contribute with the largest correlation.

5 CONCLUSION

The expected cross-correlation function of a new type of a nonparticle laser anemometer has been evaluated theoretically. The peak of the expected cross-correlation is a good measure of the mean velocity if: (1) the turbulence intensity is low ($< 10\%$); (2) the sound velocity is well separated from the convection velocity (1:2 or larger in velocity and power); and (3) the decay caused by thermal diffusion is slower than the time-of-flight. The correlation function is a complicated function of the parameters characterising the propagating and nonpropagating fluctuations.

Estimating velocity parameters should generally be done on the basis of a curve fitting procedure based on a model of the correlation function. This is in general recommendable, but is especially important when several parameters interact.

Further work is needed to investigate the validity of applying Taylor's frozen pattern hypothesis, to investigate the spectral shape of the velocity fluctuations that drives the detected refractive index fluctuations, and to evaluate the relative strength of the propagating and nonpropagating fluctuations. Concerning the actual implementation, the optics of the system described have been implemented and the first signals observed.

REFERENCES

1. Lading, L., Edwards, R. V. & Saffman, M., A phase screen approach to non-particle laser anemometry. In *Developments in Laser Techniques and Applications to Fluid Mechanics*. Springer, Berlin, 1995.
2. Lading, L., Saffman, M., Hanson, S. G. & Edwards, R. V., A combined Doppler and time-of-flight laser anemometer for measurement of density fluctuations in plasmas. *J. Atmos. Terr. Phys.*, **58** (1996) 1013–1019.
3. Lading, L., Mann, J. A. & Edwards, R. V., Analysis of a surface-scattering spectrometer. *J. Opt. Soc. Am. A.*, **6** (1989) 1692–1700.
4. Bendat J. S. & Piersol, A. G., *Random Data: Analysis and Measurement Procedures*. Wiley, New York, 1986, pp. 67–72.
5. Bird, R. B., Stewart, W. E. & Lightfoot, E. N., *Transport Phenomena*. Wiley, New York, 1960.
6. Bonnet, J. P., Grésillon, D., Cabrit, B. & Frolov, V., Collective light scattering as non-particle laser velocimetry. *Meas. Sci. Technol.*, **6** (1995) 620–636.